Chapter 1

Introduction

Magnetic topological insulators (MTIs), Weyl semimetals (WSMs), and kagome lattice materials are interconnected by the interplay of topology, symmetry breaking, and electronic correlations, giving rise to exotic quantum phenomena (Negi et al. (2025); Ning & Mao (2020)). MTIs arise when time reversal symmetry is broken in topological insulators via magnetic doping or intrinsic magnetism, leading to gapped surface states and effects like the quantum anomalous Hall effect (QAHE) (Wang et al. (2021)). WSMs arise when inversion or time reversal symmetry is broken, splitting Dirac points into Weyl nodes, which act as sources and sinks of Berry curvature, enabling unique transport effects like chiral anomaly and large anomalous Hall conductivity (Rao (2016)). Kagome lattice systems built from corner sharing triangles, naturally host flat bands, Dirac cones and topologically nontrivial states, when combined with magnetism and spin orbit coupling, produce large Berry curvature-driven phenomena, including Weyl points and quantum magnetism (Pati & Rao (2008)). Together, these materials represent a frontier in condensed matter physics, offering tunable platforms for exploring topological quantum states and potential applications in spintronics and quantum computing (Goyal et al. (2025)).

1.1 Topological Insulator

A topological insulator (TI) is a material that behaves as an insulator in the bulk but hosts conducting surface states protected by time-reversal symmetry (TRS). However, when magnetism is introduced (via doping or intrinsic magnetism), time-reversal symmetry is broken, leading to the formation of a magnetic topological insulator (MTI) (Fu et al. (2007); Tokura et al. (2019). The strong spin orbit coupling (SOC) in heavy elements (e.g., Bi, Sb, Te, Se) in TIs causes band inversion, where the conduction and valence bands swap their order at a certain momentum in the Brillouin zone. This inversion creates topologically nontrivial surface states protected by TRS. Doping in TIs (e.g., Bi_2Se_3, Bi_2Te_3, Sb_2Te_3) with transition and rare earth metals (e.g., Cr, V, Mn, Gd) introduces localized magnetic moments. These moments interact with the surface Dirac fermions via exchange interactions, breaking TRS and opening a gap at the Dirac point in the surface states (Schlenk et al. (2013)). If magnetic field is aligned perpendicular to the surface, the system exhibits QAHE, where edge channels carry dissipationless current. The Chern number depends on the nature of band inversion and exchange coupling strength. Instead of doping, some materials (e.g., $MnBi_2Te_4$, $MnSb_2Te_4$) naturally host layered antiferromagnetic (AFM) or ferromagnetic (FM) ordering, making them intrinsic MTIs (Wang et al. (2021)). Depending on layer stacking and odd/even layer thickness, it shows transition between axion insulator and QAHE states. So to understand a topological phase transition, it is essential to first grasp the concept of topology and other phenomenon related to topological insulators (Deng et al. (2020)).

1.1.1 Topology

Topology is a branch of mathematics that studies properties of spaces that remain unchanged under continuous deformations, such as stretching or bending, but not tearing or cutting. In condensed matter physics, topology plays a crucial role in classifying quantum

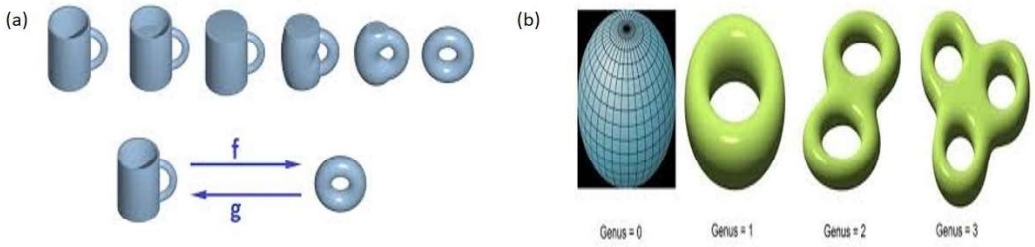

Fig. 1.1 (a) A visual representation of a continuous deformation (homeomorphism) showing how a doughnut-shaped object can be smoothly transformed into the shape of a mug, and vice versa, without cutting or gluing. (b) Classification of geometric objects according to the number of holes they contain. For instance, an object with a single hole, like a torus, is categorized as having genus 1 (Burchardt (2022)).

states of matter and understanding phase transitions that do not rely on conventional symmetry breaking but instead on changes in topological invariants (Moore (2010)). Topology in condensed matter physics is often described using the concept of the genus number (g), which represents the number of holes in a geometric object. The genus is a topological invariant, it remains unchanged under continuous deformations (stretching, bending) but changes if the structure is torn or cut. A sphere (e.g. an ordinary insulator) has genus = 0 because it has no holes. A torus (e.g., a quantum Hall system) has genus = 1 due to a single hole. A sphere and a cube are topologically equivalent because one can be continuously deformed into the other. A torus (doughnut) and a coffee mug are also topologically equivalent, as both have a single hole. However, the solid sphere and the doughnut are topologically non equivalent as the solid sphere cannot be transformed into the doughnut without creating a hole in geometry but a coffee mug can be simply transformed into the shape of a doughnut. The number of holes in an object, known as the genus, serves as a topological invariant, distinguishing different topological classes. In topology, any two objects with the same genus number (g) can be smoothly transformed into one another without altering their fundamental topological properties. This means that a surface with a single hole (such as a torus) can be continuously deformed into another surface with the

same genus without cutting, tearing or gluing preserving its topological characteristics. The mathematical framework that connects the geometry of an object (curvature) to its topology is given by the Gauss Bonnet theorem, which states:

$$\oint_M K\,dA = 2\pi\chi = 2\pi(2-2g) \tag{1.1}$$

Where, K is the Gaussian curvature at each point on the surface, dA is the infinitesimal area element of the surface M, χ is the Euler characteristic, related to the genus by χ = 2 - 2g. This theorem shows that the total curvature of a closed surface is directly related to its topology specifically, to its genus number explained in Fig. 1.1.

1.1.2 Time Reversal Symmetry (TRS):

Time reversal symmetry (TRS) plays a fundamental role in defining and protecting the topological nature of certain quantum materials, particularly topological insulators (TIs). In these materials, TRS ensures the presence of robust helical edge states or surface states, leading to unique quantum transport properties. In quantum mechanics, TRS is an anti unitary symmetry that reverses the direction of time (t $\rightarrow$ - t) and flips momentum (k $\rightarrow$ - k) and spin (S $\rightarrow$ - S). The time-reversal operator θ for spin -1/2 particles (electrons) satisfies:

$$\theta^2 = \pm 1 \tag{1.2}$$

This results in Kramers degeneracy, meaning that every electronic state at momentum k has a degenerate partner at -k with opposite spin. This degeneracy is protected as long as TRS is preserved. In topological insulators, strong spin-orbit coupling (SOC) causes band inversion, leading to the formation of Dirac-like surface states. These states exhibit spin-momentum locking, where the electron's spin orientation is determined by its momentum. The low-energy Hamiltonian of the surface states of a 3D topological insulator can be

written as

$$H_{surf} = V_F(\sigma_x k_y - \sigma_y k_x) \tag{1.3}$$

where, V_F is the Fermi velocity, σ_x, σ_y are Pauli matrices representing spin and k_x, k_y are momentum components in the 2D surface Brillouin zone (Moore (2010)). This Hamiltonian describes a massless Dirac fermion, similar to graphene, but with spin locked perpendicular to momentum. The eigenstates of this Hamiltonian lead to a helical spin texture. Electrons moving in the +x direction have spin polarized along +y. Electrons moving in the -x direction have spin polarized along -y. This results in a left handed helical spin texture around the Dirac cone. Clockwise spin for hole like states (inside Fermi surface). Counterclockwise spin for electron like states (outside Fermi surface). Thus, an electron in a TI cannot backscatter unless TRS is broken, because reversing momentum ($k \rightarrow k$) also flips the spin. Because of TRS and spin momentum locking non magnetic impurities (which do not break TRS) cannot cause 180° backscattering since such a process requires a spin flip, which is forbidden shown in Fig. 1.2. This leads to robust surface conduction even in the presence of disorder. Magnetic impurities or an external magnetic field break TRS, allowing a gap to open in the surface states and enabling backscattering. This is the basis for the Quantum Anomalous Hall Effect (QAHE) in magnetically doped TIs.

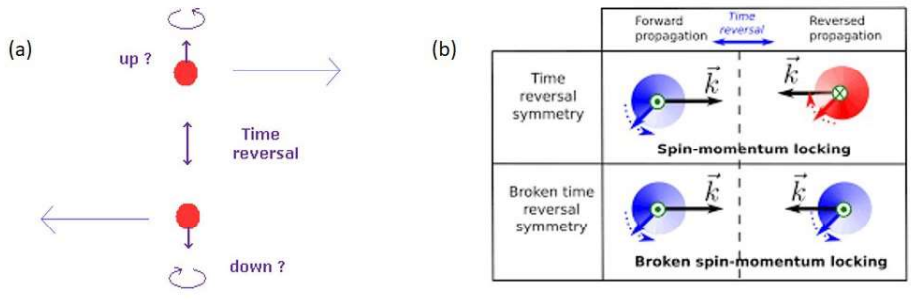

Fig. 1.2 (a) Illustration that an electron with an electric dipole moment violates time reversal symmetry. (b) Schematic of protected and broken time reversal symmetry (Rushchanskii et al. (2010)).

1.1.3 Hall Effect:

Classical Hall Effect:

The Hall effect is a fundamental phenomenon in condensed matter physics that describes the generation of a transverse voltage when an electric current flows through a conductor or semiconductor in the presence of a perpendicular magnetic field (Hall et al. (1879)). This effect is crucial for understanding charge carrier dynamics, electronic band structures, and various topological phases of matter. Consider a thin rectangular conductor (such as a metal or semiconductor) with an electric current (I) flowing along the x-axis, a magnetic field (B) applied perpendicular to the sample, along the z-axis and the formation of a Hall voltage (V_H) along the y-axis. The moving charge carriers (q) experience a Lorentz force due to the external magnetic field:

$$F = q(E + V \times B) \tag{1.4}$$

Here, E is the electric field, v is the drift velocity, and B is the magnetic field. This force deflects charge carriers towards one side of the conductor, causing charge accumulation. This accumulation builds up an electric field (E_H) along the transverse direction (y-axis), which eventually balances the Lorentz force. The equilibrium condition is reached when the Hall electric force cancels out the Lorentz force:

$$qE_H = qv_dB_q \tag{1.5}$$

Since current density is related to drift velocity as

$$J_x = nqv_d \tag{1.6}$$

we get,

$$E_H = (J_x B/nq)E_H \tag{1.7}$$

The measured Hall voltage across the width w of the sample is,

$$V_H = E_H.w = (IB/nqA).w \tag{1.8}$$

where A is the cross-sectional area. The Hall coefficient (RH) is defined as,

$$R_H = E_H/J_x = 1/nq \tag{1.9}$$

For electrons (q = -e), R_H is negative and for holes (q = +e), R_H is positive. Thus, by measuring the Hall voltage, we can determine the type (electrons or holes) and density of charge carriers in a material described in Fig. 1.3.

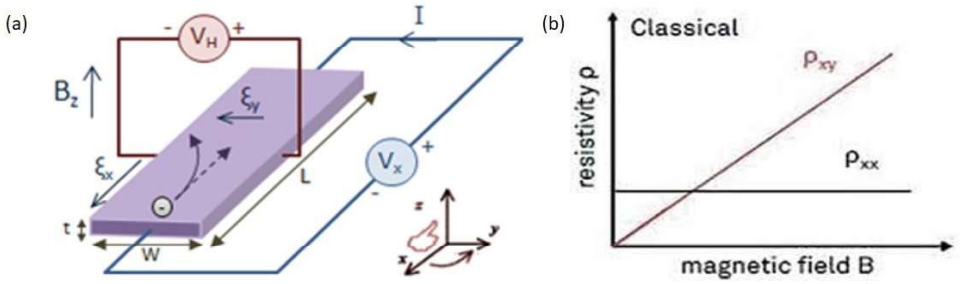

Fig. 1.3 (a) Schematic of Hall effect measurement (b) plot of longitudinal and transverse resistivity with field (Rushchanskii et al. (2010)).

Quantum Hall Effect

The Quantum Hall Effect (QHE) is a remarkable phenomenon observed in two-dimensional electron systems subjected to low temperatures and strong magnetic fields. It is characterized by the quantization of the Hall resistance (or Hall conductance) into discrete, precisely defined values, which are universal and independent of the materials. The effect has

profound implications for both fundamental physics and practical applications, such as the definition of the standard for electrical resistance. When a two-dimensional electron gas (2DEG) is subjected to a strong perpendicular magnetic field, the energy levels of the electrons quantize into discrete Landau levels. Each Landau level can hold a finite number of electrons, determined by the magnetic flux through the system. The number of occupied Landau levels is given by the filling factor $\nu = nh/eB$, where n is the electron density, h is Planck's constant, e is the electron charge, and B is the magnetic field (Cage et al. (2012)).

At certain magnetic field strengths, the Landau levels are either completely filled or completely empty. In these cases, the bulk of the material becomes insulating because there are no available states for electrons to move into within the bulk. The energy gap between Landau levels ensures that electrons cannot easily be excited to higher energy states, making the bulk resistant to conduction. While the bulk is insulating, the edges of the material can still conduct electricity. This is because the confining potential at the edges of the sample creates a spatial variation in the energy levels. Near the edges, the Landau levels bend upwards, creating states that are localized at the edges. These edge states are one-dimensional and can carry current. Electrons in these edge states move in a chiral manner (directionally dependent on the magnetic field), they only move in one direction along the edge. The edge states in the Quantum Hall regime are topologically protected. This means that their existence and properties are guaranteed by the topological nature of the bulk electronic structure, rather than by the specific details of the material or its imperfections. The topological protection arises from the fact that the bulk has a non-trivial topological invariant (Chern number) associated with its electronic band structure. This invariant ensures that the edge states are robust against local perturbations, such as disorder and imperfections, as long as the overall topology of the system remains unchanged. As a result, the edge states can conduct electricity without significant scattering, leading to quantized conductance. Because the edge states are topologically protected, they are not

easily disrupted by impurities or defects in the material. This robustness is a key feature of the Quantum Hall Effect and that is why the quantized Hall resistance is so precise and reproducible. Any backscattering (which would normally lead to resistance) is suppressed because the edge states are chiral and there are no available states for electrons to scatter into in the opposite direction explained in Fig. 1.4.

In the Quantum Hall regime, the combination of Landau level quantization and the topological nature of the electronic states leads to a situation where the bulk of the material becomes insulating, and conduction occurs only at the edges. These edge states are topologically protected, they are highly robust against disorder and imperfections, ensuring precise and quantized conductance. This unique behavior is a hallmark of the Quantum Hall Effect and has profound implications for both fundamental physics and practical applications.

Quantum Spin Hall Effect:

The Quantum Spin Hall Effect (QSHE) is a fascinating phenomenon in condensed matter physics that occurs in certain two-dimensional materials, where spin-polarized edge states conduct electricity without dissipation, while the bulk remains insulating. It is closely related to topological insulators, which are materials that exhibit unique conductive surface states protected by topology, while their bulk remains insulating (Bernevig & Zhang (2006)).

The QSHE arises due to strong spin-orbit coupling, a relativistic effect where an electron's spin interacts with its motion in a material. Spin-orbit coupling creates a separation of electron states based on their spin, leading to spin-polarized edge states. In the QSHE, the bulk of the material is insulating, but the edges host helical edge states. These are one dimensional conducting channels where electrons with opposite spins move in opposite directions. For example, spin up electrons might move clockwise along the

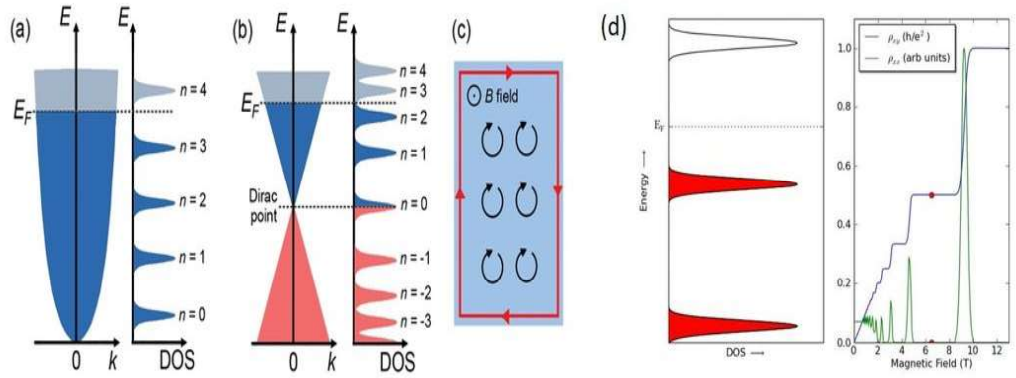

Fig. 1.4 (a, b): Illustrations of the density of states (DOS) resulting from Landau level formation in two different systems are shown. In a conventional two-dimensional electron gas (2DEG) (a) Landau levels appear as equally spaced energy states. In contrast, in systems hosting massless Dirac fermions (b) such as graphene, the energy levels scale as the square root of the Landau index n, leading to an uneven spacing of the levels. (c) Representation of the QHE under a strong magnetic field. Here, the black circular paths signify cyclotron motion of electrons localized due to the Lorentz force. The red arrows indicate chiral edge states that enable dissipationless current flow along the boundaries of the sample.(d) Depiction of Landau level evolution in the presence of a magnetic field, illustrating how longitudinal resistance and Hall resistance vary with increasing magnetic field strength, highlighting the characteristic plateaus and minima associated with QHE.(Fei et al. (2020), https://www.physicsforums.com/threads/quantum-hall-effect-resistivity.811032/).

edge, while spin down electrons move counter clockwise. The edge states are topologically protected, they are robust against non-magnetic impurities and disorder. This protection arises from the material's bulk topology, characterized by a Z_2 topological invariant. Backscattering (which would normally cause resistance) is suppressed because flipping the spin of an electron is required to scatter it into the opposite-moving state, which is difficult in the absence of magnetic perturbations. Unlike the Quantum Hall Effect, the QSHE does not require an external magnetic field. Instead, it relies on intrinsic spin-orbit coupling in the material presented in Fig. 1.5.

Topological Insulators (TIs) are materials that are insulating in their bulk but have conducting surface or edge states protected by topology. The QSHE is essentially the

2D version of a 3D topological insulator. In 2D topological insulators (which exhibit the QSHE), the edge states are spin-polarized and helical. In 3D topological insulators, the surface states form a Dirac cone, where electrons are also spin-polarized but move in all directions on the surface. Both QSHE and topological insulators are characterized by a Z_2 topological invariant, which distinguishes them from trivial insulators. The first experimental realization of the QSHE was in HgTe/CdTe quantum wells (a 2D system) in 2007 by Laurens Molenkamp and his team. A thin layer of HgTe (a semiconductor with strong spin-orbit coupling) is sandwiched between layers of CdTe (a normal semiconductor). When the HgTe layer is thicker than a critical thickness ($\approx 6.3nm$), the band structure inverts, leading to a topological phase transition. The QSHE enables the generation and control of spin currents without dissipation, which is crucial for spintronic devices and quantum computing.

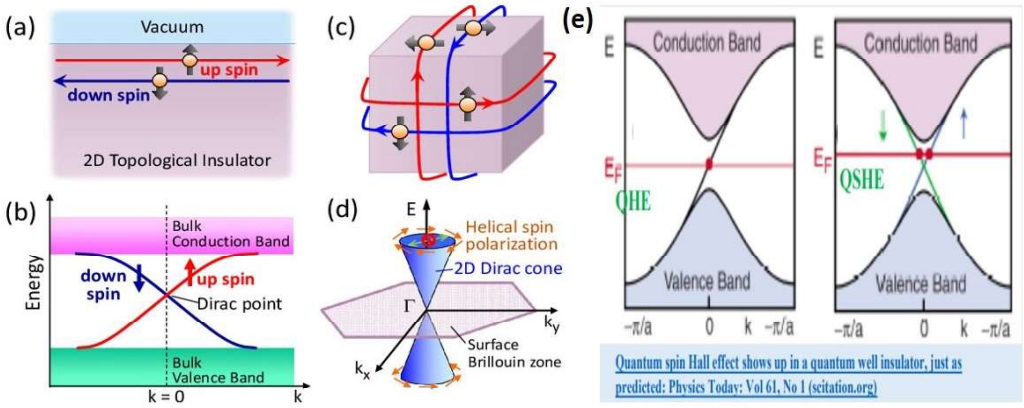

Fig. 1.5 (a–d) Conceptual illustration of the Quantum Spin Hall (QSH) effect in topological insulators. (e) (Color illustration) Depiction of helical edge states characteristic of a Quantum Spin Hall insulator (QSHI). The diagram shows the boundary between a QSHI and a conventional (trivial) insulator, where spin-polarized electrons travel along the edge. In the case of the graphene based model, spin up and spin down electrons move in opposite directions along the edges, demonstrating spin-momentum locking (Hasan & Kane (2010)).

Anomalous Hall Effect:

The Anomalous Hall Effect (AHE) is a Hall effect that occurs in magnetic materials without an external magnetic field. Unlike the ordinary Hall effect (OHE), which is due to the Lorentz force acting on charge carriers in a perpendicular magnetic field, AHE arises from the material's intrinsic electronic structure and spin orbit interactions (Nagaosa et al. (2010)). Now the total Hall resistivity is expressed as the sum of ordinary Hall resistivity (R_0H) and the anomalous Hall resistivity(R_sM); (Jungwirth et al. (2002); Wang et al. (2016b)), i.e.,

$$\rho_{xy} = R_0H + R_sM \tag{1.10}$$

Here, R_s and M are anomalous Hall coefficient and magnetization of the system, respectively (Nagaosa et al. (2010)).

- **Origins of AHE**

AHE is fundamentally caused by spin-orbit coupling (SOC) and is closely linked to the Berry curvature of electronic bands. There are three main contributions.

- **Intrinsic Mechanism (Berry Curvature Effect)**

In systems with strong spin-orbit coupling (SOC), the Berry curvature of Bloch bands acts like a momentum-space magnetic field. This modifies electron motion and causes an anomalous velocity, leading to a Hall-like response even in zero external field. The Hall conductivity in this case is related to the integral of the Berry curvature over the Brillouin zone

$$\sigma_{xy} = \frac{2\pi e^2}{h}\sum_n \int_{BZ} \frac{d^2K}{(2\pi)^2} f_n(k)\Omega_n^Z(k) \tag{1.11}$$

Where f_n (k) is the Fermi-Dirac distribution and Ω_z(k) is the Berry curvature. This mechanism is topological and does not depend on impurities.

- **Side-Jump Mechanism**

The side jump mechanism is one of the key extrinsic contributions to the anomalous Hall effect (AHE) in magnetic materials, alongside skew scattering. Unlike skew scattering, which arises from asymmetric deflection probabilities during scattering, the side jump effect originates from a lateral displacement of the electron's trajectory when it scatters off impurities or defects in the presence of spin orbit coupling. Specifically, during each scattering event, the electron's wave packet experiences a sideways shift perpendicular to both its original direction of motion and the scattering potential gradient without altering the scattering probability. This shift occurs due to the intrinsic interplay between the electron's spin and the relativistic spin orbit potential of the impurity, which breaks spatial symmetry. Importantly, the side jump contribution to the Hall conductivity is independent of the scattering rate or impurity concentration and becomes significant in clean samples where the impurity density is low but the spin–orbit interaction remains strong. In the broader context of AHE, the side jump effect highlights how spin–orbit coupling can induce transverse electronic transport not just through the Berry curvature of the band structure (intrinsic AHE) but also via real space displacements during scattering events.

- **Skew Scattering Mechanism**

The skew scattering mechanism is an extrinsic process that contributes to the anomalous Hall effect (AHE) in ferromagnetic and spin orbit coupled materials. It arises when conduction electrons scatter asymmetrically off impurities or defects due to the presence of spin–orbit interaction. Unlike normal (isotropic) scattering, which deflects electrons symmetrically around the impurity, the spin orbit coupling creates a spin-dependent force that causes electrons to preferentially scatter more to one side, leading to a net transverse deflection relative to the applied electric field. This asymmetric scattering results in a build-up of charge carriers on one side of the sample, producing a measurable transverse (Hall) voltage even in the absence of an external magnetic field. The strength of the skew scattering contribution is directly proportional to the scattering time (τ), meaning it becomes more dominant in cleaner samples with fewer impurities (longer τ), where electrons can travel longer before scattering. Skew scattering reflects the direct microscopic

consequence of how spin orbit coupling links an electron's spin orientation to its real-space trajectory during impurity interactions, and it remains one of the hallmark extrinsic mechanisms behind the anomalous Hall effect presented in Fig. 1.6.

- **Anomalous Hall Conductivity**

The total anomalous Hall conductivity

$$\sigma_{xy}^{\text{AHE}} = \sigma_{xy}^{\text{intrinsic}} + \sigma_{xy}^{\text{side-jump}} + \sigma_{xy}^{\text{skew-scattering}} \tag{1.12}$$

At very low impurity concentrations, skew scattering dominates ($\sigma_{xy} \sim 1/\rho_{xx}$). At moderate disorder, side-jump and intrinsic effects dominate ($\sigma_{xy} \sim constant$). At very high disorder, scaling laws break down. In magnetic topological insulators, Berry curvature is enhanced by band inversion, leading to large AHE. AHE occurs in ferromagnets without an external field, driven by SOC and Berry curvature. It has intrinsic (Berry curvature), side jump, and skew scattering contributions. It plays a crucial role in topological materials, leading to exotic transport phenomena.

Topological Hall Effect:

The Topological Hall Effect (THE) is an additional Hall effect that arises when conduction electrons move through a noncoplanar spin texture, such as skyrmions, in magnetic materials. Unlike the Ordinary Hall Effect (OHE) (caused by external magnetic fields) and the Anomalous Hall Effect (AHE) (due to spin orbit coupling and Berry curvature), THE is caused by an emergent magnetic field originating from real space spin configurations (Wang et al. (2022)).

In a system with a non trivial spin texture, electrons experience an effective magnetic field in real space, leading to a Hall voltage. This is known as the spin Berry phase mechanism. When an electron moves through a material with a non-coplanar spin texture, its spin aligns adiabatically with the local magnetic moments. As the electron's spin follows

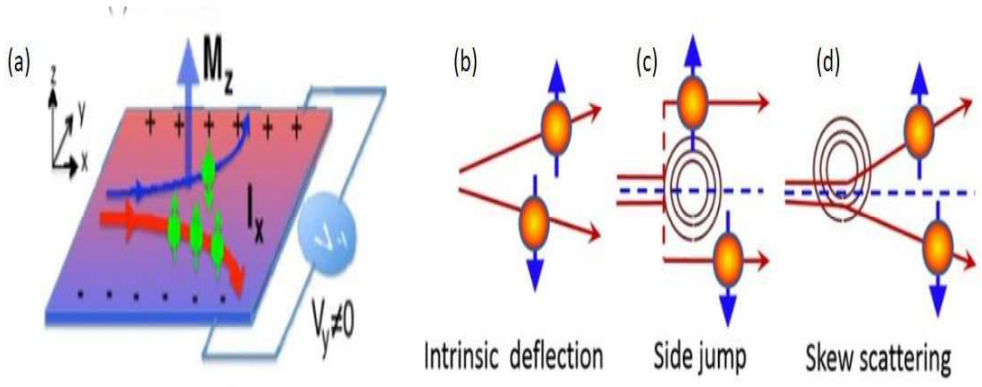

Fig. 1.6 (a): Illustration of the Anomalous Hall Effect (AHE). In the presence of spontaneous magnetization along z axis (M_z) electrons with opposite spin orientations experience different transverse (anomalous) velocities due to spin orbit interaction. This results in an asymmetric distribution of charge carriers across the sides of the material, producing a measurable Hall voltage (V_y) even without an external magnetic field. (b) Conceptual diagram showing the two primary origins of the AHE: the intrinsic mechanism, arising from the Berry curvature of the band structure, and the extrinsic mechanisms, which include skew scattering and side-jump processes caused by impurity scattering. (Weng et al. (2015); Zhu & Zhao (2017)).

this texture, it picks up a real-space Berry phase. This phase acts like an effective magnetic field, which deflects electrons transversely, causing a Hall voltage. This mechanism is distinct from the Berry curvature driven AHE, which is due to momentum space effects shown in Fig. 1.7.

1.1.4 Band Inversion:

The band inversion mechanism is the key concept that distinguishes a topological insulator (TI) from a conventional insulator. It occurs when the ordering of electronic energy bands is reversed due to strong spin-orbit coupling (SOC), leading to the emergence of topologically protected surface states. In a normal insulator, the valence band (dominated by anion orbitals) lies below the conduction band (dominated by cation orbitals), separated by an energy gap but in a topological insulator, strong SOC causes the valence and conduction bands to invert at certain points in momentum space, leading to a nontrivial topological

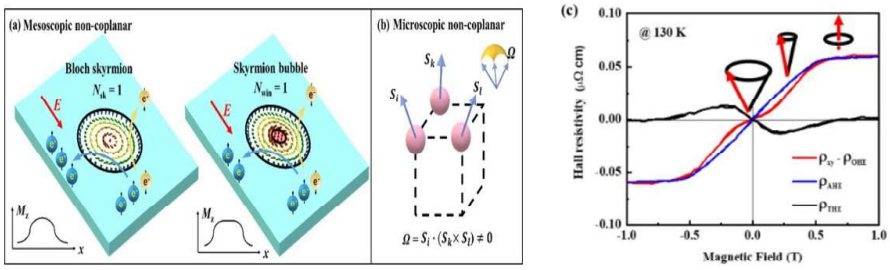

Fig. 1.7 (a) One origin of the Topological Hall Effect (THE) arises from a non-coplanar spin configuration at the atomic scale. The schematic illustrates three neighboring spins S_i, S_k, and S_l forming a finite solid angle Ω, which generates an emergent magnetic field acting on conduction electrons. (b) Another source of THE is related to the real-space topology of the spin texture. In systems hosting skyrmions or skyrmion bubbles, the swirling spin structure leads to asymmetric deflection of spin-polarized electrons, contributing to a transverse voltage. The inset presents the spatial variation of the out of plane magnetization M_z along the in plane x direction, illustrating the internal structure of these textures.(c) Experimental plot showing the variation of topological Hall resistivity as a function of the applied magnetic field, highlighting the presence of THE in a specific field window (He et al. (2022)).

phase. In heavy elements (e.g., Bi, Sb, Te, Se), SOC is strong and modifies the band structure. SOC mixes spin and orbital degrees of freedom, leading to splitting and shifting of electronic bands. In conventional semiconductors, the conduction band has s orbital character, while the valence band has p orbital character. In topological insulators, SOC reverses this order. The p-orbital states move above the s orbital states at certain points (e.g. Γ-point in the Brillouin zone). This results in an inverted band structure, where the usual conduction band now acts as the valence band and vice versa (Zhu et al. (2012)). The band inversion leads to the emergence of gapless Dirac like surface states at the interface between a TI and a normal insulator (or vacuum). These topological surface states are protected by time-reversal symmetry (TRS) and exhibit a helical spin momentum locking structue explained in Fig. 1.8. The band inversion mechanism in topological insulators arises due to strong SOC, leading to a nontrivial band topology and protected surface states. This phenomenon underlies many exotic quantum effects, such as the quantum spin Hall

effect, spin momentum locking, and topological superconductivity, making TIs crucial for future quantum computing and spintronic applications.

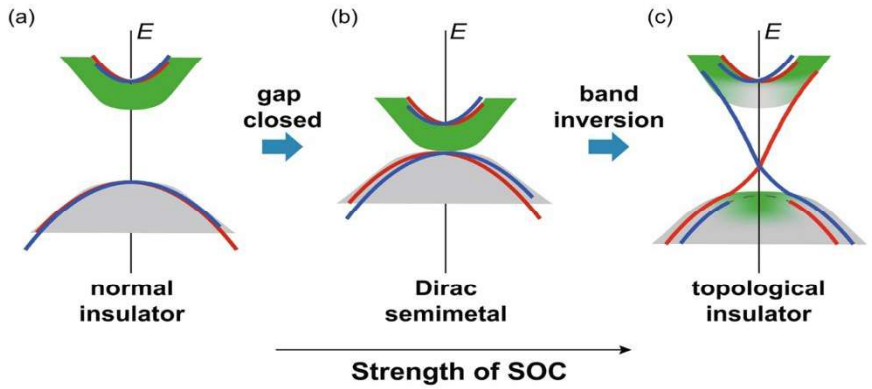

Fig. 1.8 (a–c) Conceptual representation of a topological phase transition. The sequence shows the transformation of the electronic band structure from a conventional insulating state (a) progressing through a gapless Dirac semimetal state (b) and eventually reaching a topological insulator phase (c) where band inversion occurs due to strong spin orbit coupling.(Yaji et al. (2024)).

1.1.5 Concept of Berry Phase:

Berry phase and Berry curvature are fundamental concepts in the study of topological insulators (TIs), providing a deep understanding of their electronic properties, quantum transport phenomena, and topological invariants (Manoharan (2010); Xiao et al. (2010)). The Berry phase is a geometric phase acquired by a quantum system when its wavefunction evolves adiabatically around a closed loop in parameter space. Unlike the dynamical phase, which depends on time and energy, the Berry phase arises purely due to the geometry of the wavefunction evolution. One of the best classical analogies to understand Berry phase is the Foucault pendulum. If you set up a pendulum at the North Pole, it keeps swinging in the same plane while the Earth rotates beneath it. However, at lower latitudes, the pendulum's oscillation plane slowly rotates due to the curvature of the Earth's surface. The amount by which the pendulum's plane rotates depends only on the latitude and not on the

speed of rotation. This rotation is analogous to the Berry phase, a phase shift that depends on the curvature of the underlying space. Similarly, in quantum mechanics, if a system's parameters move along a closed loop in parameter space, its wave function acquires an additional phase the Berry phase which depends on the geometry of the parameter space.

Consider an electron in a material. Its quantum state is represented by a Bloch wavefunction $u_n(k)$, which evolves as the crystal momentum k changes. If we slowly move k around a closed loop, the wavefunction doesn't return exactly to its original state it picks up a Berry phase. This phase shift is independent of the time taken to complete the loop. It arises due to the internal structure (curvature) of the wavefunction space. Imagine a vector on the surface of a sphere. If you move it in a closed path without allowing it to "twist" relative to the surface, it may still come back rotated compared to its initial direction. This mismatch is the Berry phase in quantum mechanics. If an electron moves around a magnetic flux tube, even if the magnetic field is confined inside, the electron acquires a phase shift due to the vector potential. This is a direct manifestation of Berry phase. In materials with strong spin-orbit coupling, the Berry curvature acts like a momentum-space magnetic field. This causes an intrinsic Hall Effect even without an external magnetic field. The nontrivial Berry phase (often) ensures that surface states in a topological insulator remain gapless presented in Fig. 1.9. This leads to robust edge/surface transport.

1.1.6 Magnetoresistance:

Magnetoresistance (MR) is the change in electrical resistance of a material when an external magnetic field is applied. It is a fundamental transport property used to study charge carrier dynamics, band structure, and topological effects in various materials, including topological insulators, Weyl semimetals, and magnetic materials (Pippard (1989)). The resistance of a

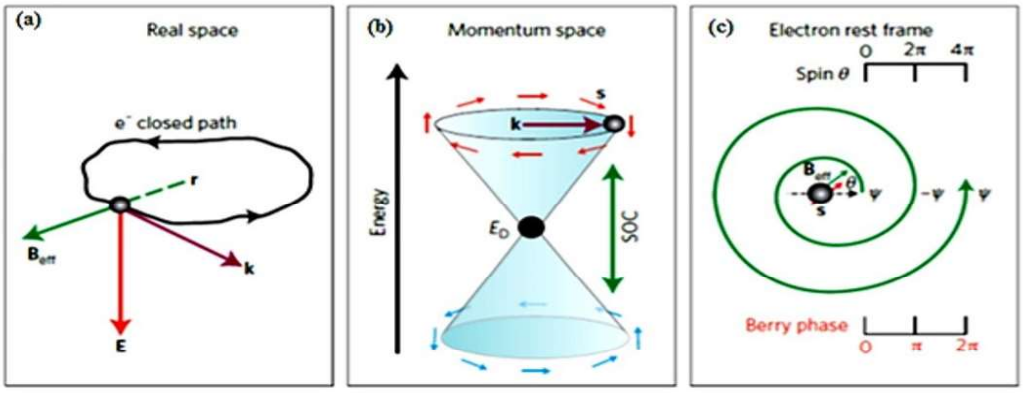

Fig. 1.9 (a) The real space picture of electron's orbit (b) Formation of the Dirac cone due to SOC in momentum space (c) Berry phase and change in electron's wave function in its rest frame (Manoharan (2010)).

material in the presence of a magnetic field B is given by,

$$MR\% = \frac{R(B) - R(0)}{R(0)} \times 100\% \tag{1.13}$$

Where, R(B) is the resistance with applied magnetic field and R(0) is the resistance without a magnetic field. If MR > 0, resistance increases with the magnetic field (positive MR). If MR < 0, resistance decreases with the magnetic field (negative MR).

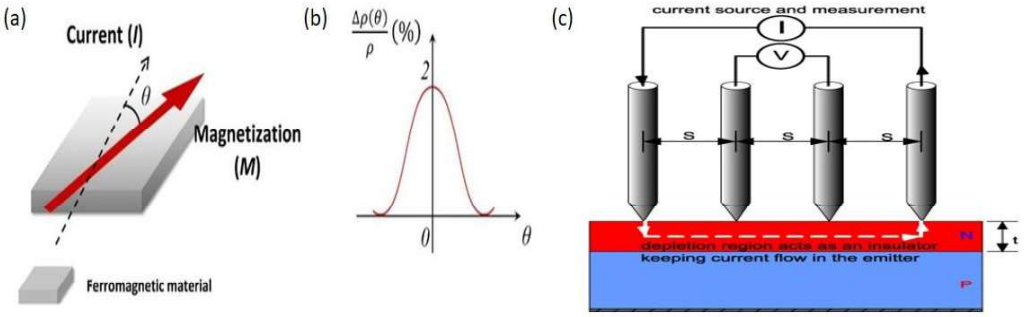

Fig. 1.10 (a, b) Schematic diagram of anisotropic magnetoresistance (AMR).(b) Schematic of four probe measurement of MR (Yang & Zhang (2021)).

1.1.7 Shubnikov–de Haas Oscillations:

Shubnikov–de Haas (SdH) oscillations are quantum oscillations observed in the electrical resistivity (ρ_{xx}) of a material when subjected to a strong magnetic field at low temperatures. These oscillations arise due to the Landau quantization of electronic states and provide key insights into a material's Fermi surface, effective mass, carrier density, and quantum transport properties. In presence of a perpendicular magnetic field B, the continuous energy spectrum of electrons in a metal or semiconductor splits into discrete Landau levels (LLs),

$$E_n = (n + \frac{1}{2})\frac{h}{2\pi}\omega_c \tag{1.14}$$

Where, n = 0, 1, 2,... n is the Landau level index. $\frac{h}{2\pi}$ is the reduced Planck's constant. $\omega_c = eB/m^*$ is the cyclotron frequency and m* is the effective mass of charge carriers. The density of states (DOS) in a magnetic field becomes oscillatory, as electronic states are now confined into Landau levels. As B increases, the separation between Landau levels grows, and they pass through the Fermi level (E_F). When a Landau level is completely filled, the system has a lower resistivity. When a Landau level is partially filled, increased scattering leads to higher resistivity (Shoenberg (2009)). This periodic filling and emptying of Landau levels cause oscillations in the resistivity as a function of 1/B. The SdH oscillations follow the Lifshitz-Kosevich (LK) formula:

$$R_{xx} \propto R_T R_D cos[2\pi(n + 1/2 - \phi_B/2\pi - \delta)]. \tag{1.15}$$

$$Where, R_T = \frac{(\alpha T m^*/H)}{[sinh(\alpha T_D m^*/H)]} \tag{1.16}$$

$$R_D = exp(-\alpha T_D m^*/H) \tag{1.17}$$

Here,$\alpha = \frac{4\pi^3 k_B m^*}{eh}$ is a constant, m is the effective mass of the charge carriers, R_{xx} is the longitudinal resistance, RT and R_D are defined as the thermal damping factor and Dingle

factor and T_D is the Damping temperature. $F = (/2\pi e)A_F$ is the oscillation frequency, related to the cross-sectional area of the Fermi surface $A_F = \pi(k_F)^2$. ϕ is a phase factor, related to Berry phase effects. In Topological materials (e.g. Topological insulators, Weyl semimetals) exhibit a non-trivial Berry phase (π), detected by SdH phase analysis.

1.2 Weyl Semimetals (WSMs)

A Weyl semimetal (WSM) is a gapless topological phase where conduction and valence bands touch at isolated points (Weyl nodes), which act as monopoles of Berry curvature. These materials break either inversion symmetry (IS) or time-reversal symmetry (TRS), leading to exotic transport and optical phenomena (Yan & Felser (2017)). In a conventional Dirac semimetal (e.g., Na_3Bi, Cd_3S_2), each Dirac point consists of two degenerate Weyl nodes due to TRS and IS. To split a Dirac point into two non-degenerate Weyl nodes, at least one symmetry must be broken. Breaking IS (e.g., TaAs, NbP) shifts Weyl nodes in momentum space and breaking TRS (e.g., $Co_3Sn_2S_2$, magnetic WSMs) splits Weyl nodes in energy. These Weyl nodes always appear in pairs of opposite chirality (+1 and -1 monopoles of Berry curvature) (Huang et al. (2015); Muechler et al. (2020)). They cannot be annihilated unless brought together in momentum space. Unlike topological insulators with closed surface Dirac cones, WSMs host open Fermi arcs, connecting Weyl nodes of opposite chirality across the surface Brillouin zone. These weyl semimetals are important due to their unique Anomalous Transport Signatures like Chiral anomaly which leads Charge pumping between Weyl nodes under parallel electric and magnetic fields and large magnetoresistance and anomalous Hall effect arising from Berry curvature effects. Magnetic order can split or shift Weyl nodes, leading to new phases like type-II Weyl semimetals (e.g., WTe_2) and Weyl ferromagnets (e.g., $Co_3Sn_2S_2$, Fe_3Sn_2). The concept of Weyl semimetals emerged from theoretical physics and condensed matter studies. Weyl semimetals are materials where the low-energy excitations behave like Weyl

fermions—massless particles with a definite chirality. These materials exhibit unique properties, such as linear energy dispersion and topologically protected surface states known as Fermi arcs. The theoretical prediction of Weyl fermions in condensed matter systems dates back to Conyers Herring in 1937, but it wasn't until much later that real materials exhibiting these properties were discovered. Crystalline tantalum arsenide (TaAs) was the first experimentally confirmed Weyl semimetal. The Dirac equation was introduced by Paul Dirac in 1928 as a relativistic version of the Schrödinger equation. It describes particles (like free electrons and positrons) that possess mass and have four components due to the Dirac spinor representation. In condensed matter systems, this equation can be adapted to describe electrons in solid materials, where the mass term corresponds to the energy gap in the band structure. The dispersion relation is given by:

$$E = \sqrt{P_x^2 + P_y^2 + P_z^2 + m^2} \tag{1.18}$$

Here, m is the mass of the fermion. Hermann Weyl extended this work in 1929 by solving the Schrödinger equation under the condition that the particles are massless. Weyl fermions have only two components due to the use of Pauli matrices ($\sigma_x, \sigma_y, \sigma_z$), instead of the four-component Dirac matrices. The Weyl equation leads to the following Hamiltonian and energy dispersion:

$$H = \sigma_x p_x + \sigma_y p_y + \sigma_z p_z \tag{1.19}$$

$$E = \sqrt{p_x^2 + p_y^2 + p_z^2} \tag{1.20}$$

Since the Pauli matrices couple directly to momentum (p_x, p_y, p_z), there is no term for mass, meaning the bands are gapless. In solids, Weyl fermions manifest as quasiparticles within materials exhibiting the so-called Weyl semimetal phase. WSMs have a linear energy dispersion and exhibit stable "gapless points" in their band structure, known as Weyl nodes. These nodes occur in pairs of opposite chirality and are robust due to their

topological nature disturbances cannot easily open a gap at these points. To summarize, the Weyl semimetal phase is a 3D phase of matter characterized by gapless points and linear energy dispersion, arising from the massless nature of Weyl fermions. These materials have exciting properties like Fermi arcs and exceptional electronic behavior, which could lead to futuristic applications in quantum computing and electronics shown in Fig. 1.11.

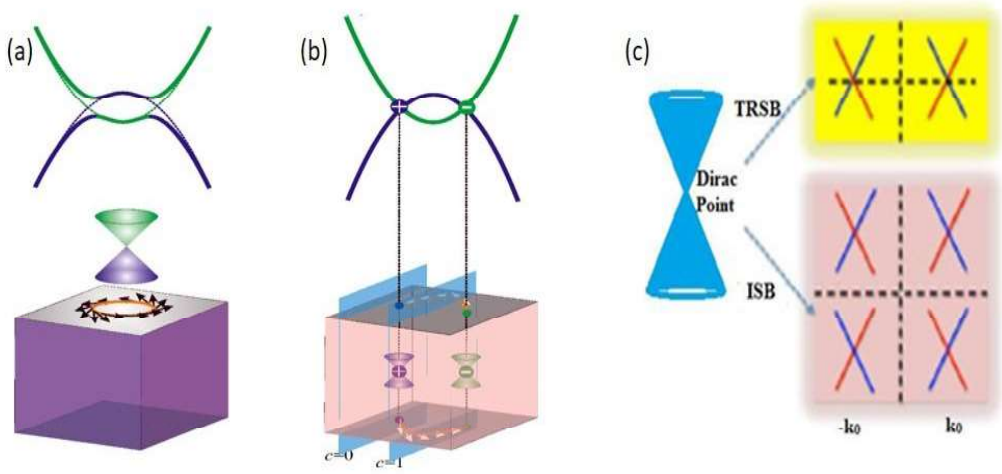

Fig. 1.11 Schematics of the topological insulator and Weyl semimetal. (a) A TI exhibits an energy gap with a band inversion. Topological surface states exhibits Dirac-cone-type dispersion with spin texture. (b) A WSM is gapless in the bulk and a pair of Weyl points (band crossing points) exists with opposite parity. Nonzero Chern number (c) Schematics of Dirac point splitting into separated Weyl points upon breaking TRS and IS (Sun et al. (2015)).

1.2.1 Chiral anomaly and chirality:

In Weyl semimetals, electrons behave as massless Weyl fermions, which possess a quantum property known as chirality. Chirality refers to whether the spin of a Weyl fermion is aligned (right handed) or anti aligned (left handed) with its momentum. In momentum space, Weyl nodes, which act as sources or sinks of Berry curvature, always appear in pairs with opposite chirality due to the Nielsen-Ninomiya theorem. In the presence of an external electric field (E) and magnetic field (B), a phenomenon known as the chiral

anomaly emerges: when E||B, charge is pumped between Weyl nodes of opposite chirality, leading to a breakdown of separate conservation of left and right chiral fermions. This quantum mechanical effect results in negative longitudinal magnetoresistance (NMR) instead of resistance increasing with magnetic field (as in conventional materials), it decreases due to the enhanced charge transport along the field direction. This anomaly is a condensed matter realization of the Adler Bell Jackiw anomaly in quantum field theory, bridging high energy physics and condensed matter (Zyuzin & Burkov (2012)). The chiral anomaly has been experimentally confirmed in Weyl semimetals such as TaAs, NbP, and Cd_3As_2 via magnetotransport measurements.

1.2.2 Broken symmetry:

Weyl semimetals arise when a Dirac point (which is a fourfold degenerate crossing of two doubly degenerate bands) splits into two non-degenerate Weyl nodes due to the breaking of either inversion symmetry (IS) or time-reversal symmetry (TRS). If inversion symmetry is broken, as in TaAs, NbP, and $MoTe_2$, the Weyl nodes appear at different energy levels and momenta in the Brillouin zone, leading to an asymmetric electronic dispersion. This results in non-centrosymmetric Weyl semimetals, where the lack of a spatial inversion center shifts Weyl nodes away from symmetric positions. On the other hand, if time-reversal symmetry is broken, as in magnetic Weyl semimetals like $Co_3Sn_2S_2$ and Mn_3Sn, an intrinsic magnetization or spin ordering lifts the Kramers degeneracy and separates Weyl nodes with opposite chirality. This results in strong Berry curvature effects, giving rise to anomalous Hall conductivity (AHC) and the topological Hall effect (THE). In some cases, both TRS and IS can be broken simultaneously, further enriching the topological phase diagram by enabling new states like axion insulators and Weyl superconductors. Thus, the nature of broken symmetry fundamentally determines the location, energy, and

number of Weyl nodes, which in turn govern the exotic quantum and transport phenomena observed in Weyl semimetals (Zyuzin et al. (2012)).

1.2.3 Different types of Weyl Semimetal:

Type-I Weyl semimetals have well-separated Weyl nodes with a linear dispersion resembling the relativistic Weyl equation. The Fermi surface consists of discrete points where conduction and valence bands touch. They exhibit the chiral anomaly and negative longitudinal magnetoresistance (NMR). The Berry curvature near Weyl nodes leads to strong anomalous Hall conductivity.

Examples: TaAs, NbP, WTe_2 (in certain phases)

Type-II Weyl semimetals arise when tilted Weyl cones appear due to strong spin-orbit coupling and electronic band structure distortions. Unlike Type-I, their Weyl nodes exist at the boundary of electron and hole pockets, leading to an open Fermi surface. They host highly anisotropic magnetotransport properties due to the coexistence of electrons and holes at the Fermi level. The chiral anomaly effects are present but modified by the tilted dispersion depicted in Fig. 1.12 (Morishima & Kondo (2021)).

Examples: WTe_2, $MoTe_2$, LaAlGe.

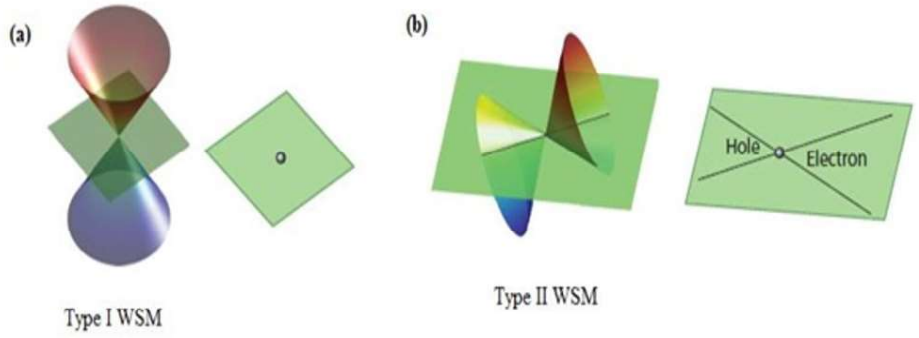

Fig. 1.12 types of Weyl semimetal (a) Type I weyl semimetal (b) Type II weyl semimetal (Rodriguez-Lopez et al. (2020)).

1.3 Kagome Lattice Materials

The kagome lattice is a 2D network of corner-sharing triangles, leading to flat bands, Dirac cones, and topological states due to destructive quantum interference and geometric frustration. The triangular network leads to localized electronic states forming a nearly dispersionless flat band, which enhances electron correlation effects (Wang et al. (2024). In these materials Dirac cones naturally emerge due to the hexagonal symmetry. In heavy-element kagome compounds (e.g., Fe_3Sn_2, $Co_3Sn_2S_2$), SOC induces spin-polarized topological states with large Berry curvature, leading to Anomalous Hall Effect (AHE), Orbital magnetism, Chiral edge modes in magnetic kagome systems. In magnetic Kagome Metals when combined with ferromagnetism, kagome systems exhibit Weyl points and flat band magnetism (Kanagaraj et al. (2022); Zhang et al. (2022a)). This leads to large intrinsic anomalous Hall conductivity and potential for quantum anomalous Hall states. In Some kagome systems ((e.g., CsV_3Sb_5, KV_3Sb_5) exhibit unconventional superconductivity with intertwined charge density wave (CDW) and topological pairing mechanisms explained in Fig. 1.13.

1.4 Skyrmions:

A skyrmion is a topologically protected, vortex-like spin texture that appears in certain magnetic materials. It represents a swirling configuration of local magnetic moments (spins), where the spins gradually rotate from one orientation at the core to another at the boundary. Skyrmions are nanoscale in size (typically 1–100 nm) and behave like quasiparticles that can be moved with extremely low electrical currents, making them promising for spintronic applications. Skyrmions form a non-trivial spin configuration, meaning that the spin direction continuously varies in space, unlike simple ferromagnets where all spins are aligned. The core of the skyrmion usually points upward (+z direction),

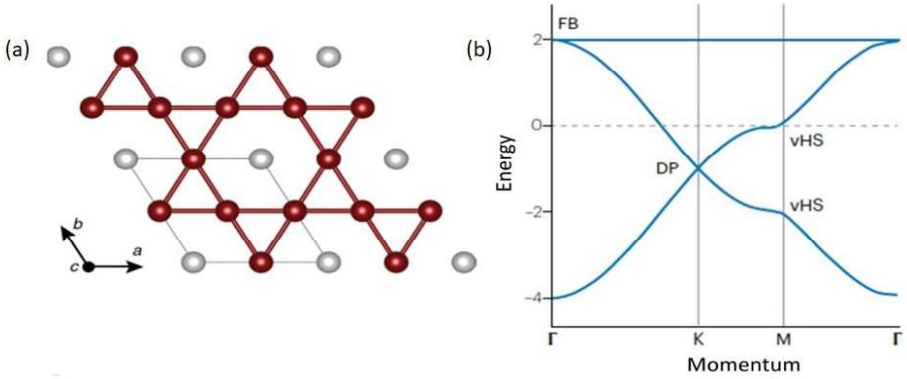

Fig. 1.13 (a) The kagome lattice is a two-dimensional structure composed of corner-connected triangles, often likened to the shape of a 'David star' or traditional Japanese basket-weaving motifs. (b) This lattice possesses unique symmetry properties that give rise to two contrasting electronic features: massless Dirac fermions with zero effective mass, and completely flat energy bands with no dispersion, corresponding to infinitely heavy quasiparticles.(https://scattering.mit.edu/research-areas).

while the outer spins point downward (-z direction), or vice versa. The winding number (or topological charge, Q) quantifies the number of times the spin field wraps around the unit sphere

$$Q = \frac{1}{4\pi}\int n.(\frac{\delta n}{\delta x} - \frac{\delta n}{\delta y})\delta x \delta y \tag{1.21}$$

Skyrmions emerge due to competition between different magnetic interactions like Dzyaloshinskii-Moriya Interaction (DMI) which arises from spin-orbit coupling in non-centrosymmetric materials (e.g., B_{20} compounds like MnSi and FeGe). It favors a twisting spin configuration, stabilizing skyrmions in materials with broken inversion symmetry. Long-range dipole-dipole interactions can also stabilize skyrmions in some materials like Co-based thin films. Applying an external magnetic field or varying temperature can stabilize or control skyrmions presented in Fig. 1.14 (Fert et al. (2017)).

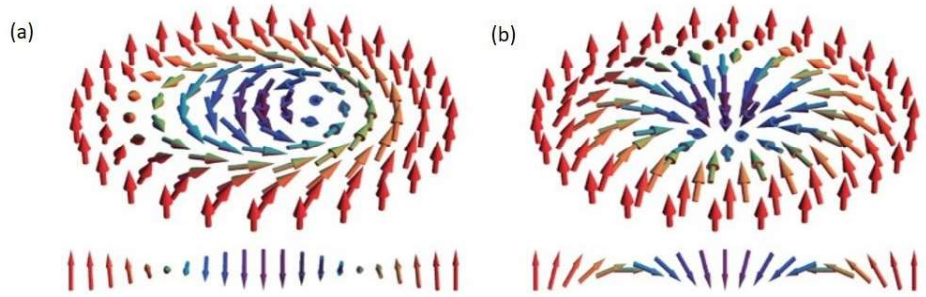

Fig. 1.14 (a) In a Bloch type skyrmion, spin orientations twist within planes that are tangential to concentric circles around the core—meaning the spins rotate perpendicular to the radial direction as one moves outward from the center. (b) For a Néel type skyrmion, spins rotate within radial planes, aligning from the center outward in a pattern resembling spokes on a wheel. Cross sectional views of the spin textures are shown for both types, illustrating their distinct vortex structures(Kézsmárki et al. (2015)).

1.4.1 Types of Skyrmions:

Bloch type skyrmion (Vortex like spin texture) which found in B_{20} compounds (MnSi, FeGe). Néel type skyrmion (Hedgehog like spin texture) found in thin films with interfacial DMI (Pt/Co/Ir multilayers). Antiskyrmions which found in some Heusler compounds, with opposite winding compared to skyrmions presented in Fig. 1.15 (Felser (2013)).

Skyrmions are fascinating topological spin textures that offer new avenues for energy efficient spintronics, nonvolatile memory, and topological quantum computing. Their unique transport properties, stability, and small size make them highly promising for next generation nanoelectronic devices.

The emergence of magnetic topological insulators, Weyl semimetals, and kagome lattice materials is deeply rooted in the interplay of topology, symmetry breaking, and strong electronic correlations. These materials offer rich physics, from QAHE and chiral edge transport in MTIs, to exotic magnetotransport and chiral anomaly in WSMs, to flat band physics and frustrated magnetism in kagome lattices. Their study is crucial for future quantum technologies, including spintronics and topological quantum computation.

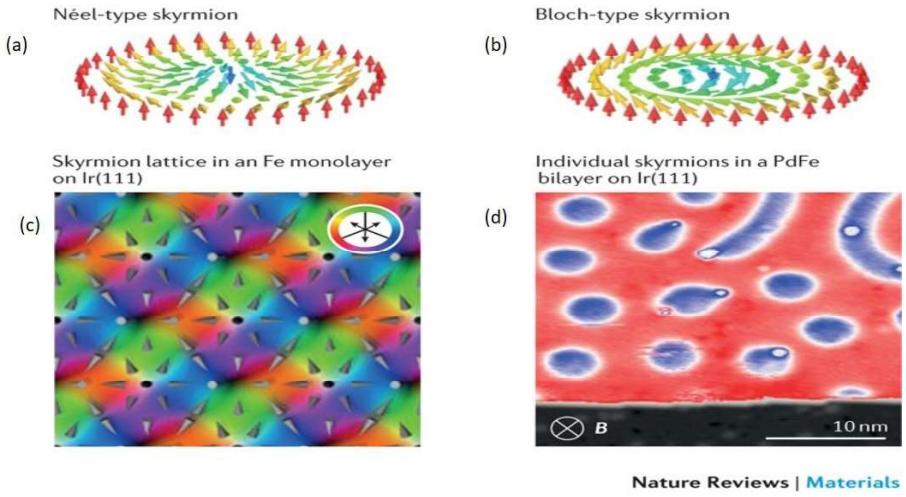

Fig. 1.15 (a, b) Illustrations of Néel type (a) and Bloch type (b) skyrmions, where the magnetization transitions from pointing downward at the core to aligning upward at the edge, consistent with the surrounding uniform magnetic field. This behavior mirrors that of Néel and Bloch domain walls, respectively.(c) A skyrmion lattice imaged using spin polarized scanning tunneling microscopy (SP-STM) in a single atomic layer of Fe deposited on an Ir(111) substrate. The color wheel represents the orientation of the in-plane magnetization, and the square unit cell of the lattice has a side length of 1 nm. Grey cones show the full 3D orientation of magnetic moments. (d) Isolated skyrmions detected by the same SP-STM technique in a bilayer of PdFe on Ir(111), highlighting their individual magnetic structure. (Fert et al. (2017)).

1.5 Objective of Present Thesis:

The primary objective of this research is to synthesize and investigate various quantum materials, specifically magnetic topological insulators (MTIs), Weyl semimetals (WSMs), and kagome lattices, focusing on their physical, magnetic, and thermoelectric properties. Initially, this work explores 3D single-crystalline magnetic topological insulators by introducing a minimal concentration of magnetic dopants to examine their impact on topological surface states, magneto-transport properties, and quantum anomalies. Additionally, we have synthesized 3D intrinsic MTI to study the effects of magnetic and transport properties and the doping effects on the topological phase, aiming to manipulate spin dynamics at the interface. Furthermore, a ferromagnetic Weyl semimetal (WSM) is synthesized to realize

topologically protected Weyl nodes and their interplay with transport properties. Special emphasis is placed on achieving a Skyrmion-like vortex magnetic phase in a specific temperature range, enhancing Skyrmion stability via chemical pressure through elemental substitution. Lastly, kagome-based topological magnets are explored to understand their intrinsic Berry curvature effects, large anomalous Hall conductivity, and unconventional magnetic phases, paving the way for novel quantum phenomena and potential spintronic applications.